PROCEEDINGS OF SCIENCE

Global properties in O+O collisions at $\sqrt{s_{\rm NN}}$ = 7 TeV using AMPT model

Debadatta Behera,[a,*] Neelkamal Mallick,[a] Sushanta Tripathy,[b] Suraj Prasad,[a] Aditya Nath Mishra[c] and Raghunath Sahoo[a,d]

[a] *Department of Physics, Indian Institute of Technology Indore, Simrol, Indore 453552, India*
[b] *INFN - sezione di Bologna, via Irnerio 46, 40126 Bologna BO, Italy*
[c] *Wigner Research Center for Physics, H-1121 Budapest, Hungary*
[d] *CERN, CH 1211, Geneva 23, Switzerland*
E-mail: debadatta.behera@cern.ch, neelkamal.mallick@cern.ch, sushanta.tripathy@cern.ch, suraj.prasad@cern.ch, aditya.nath.mishra@cern.ch, raghunath.sahoo@cern.ch

Extensive research on heavy-ion collisions at the Large Hadron Collider (LHC) and Relativistic Heavy Ion Collider (RHIC) has helped us produce and study the properties of quark-gluon plasma (QGP). Recent investigations hint towards the possible formation of QGP-droplets even in small collision systems such as high-multiplicity pp collisions. Oxygen-Oxygen (O+O) collisions are expected in the forthcoming RUN3 at the LHC. This will provide an essential and timely opportunity to investigate the effects of high-multiplicity pp and p+Pb collisions with similar system sizes. In this work, we implement harmonic oscillator and Woods-Saxon type density profiles for the oxygen nucleus. Also, an alpha-cluster tetrahedral structure for the oxygen nucleus is studied. We report the charged-particle multiplicity, transverse mass, Bjorken energy density, squared speed of sound, and the kinetic freezeout parameters in O+O collisions at $\sqrt{s_{\rm NN}}$ = 7 TeV using a multiphase transport model.

The Tenth Annual Conference on Large Hadron Collider Physics - LHCP2022
16-20 May 2022
online

*Speaker

© Copyright owned by the author(s) under the terms of the Creative Commons Attribution-NonCommercial-NoDerivatives 4.0 International License (CC BY-NC-ND 4.0).

https://pos.sissa.it/

PoS(LHCP2022)305

1. Introduction

The primary objective of heavy-ion collisions at relativistic energies is to study quark-gluon plasma formation (QGP) by creating extreme temperature and energy density conditions. Several measurements in various collision systems at different center-of-mass energies at the Large Hadron Collider (LHC) and Relativistic Heavy Ion Collider (RHIC) are studied to understand the characteristics of this hot and dense nuclear matter. Heavy-ion collisions like Pb+Pb and Au+Au have historically been the main focus of QGP research, while small collision systems like proton-proton (pp) serve as a baseline.

A short run for Oxygen-Oxygen (O+O) collisions are anticipated in RUN3 at the LHC [1]. Oxygen has final state multiplicity overlap with pp, p+Pb, and Pb+Pb collisions. It may be easier to comprehend the QGP-like characteristics in small collision systems if systems created in O+O collisions are studied in depth. It can also help understand the source of collectivity in small collision systems. A multiphase transport model (AMPT) [2] has been used to accommodate both the harmonic oscillator (HO) density profile and the more realistic Woods-Saxon (WS) density profile in the oxygen nucleus along with an α-clustered structure (α-C). The potential production of QGP medium can be inferred from the global observables such as charged-particle multiplicity, transverse energy, particle spectra, and pseudorapidity distributions. This study uses AMPT to examine Bjorken energy density, squared speed of sound, and kinetic freezeout parameters, in O+O collisions at $\sqrt{s_{\rm NN}}$ = 7 TeV.

2. Results and discussions

One of the most important factors for the formation of QGP in heavy-ion collisions is the initial energy density. The Bjorken boost-invariant hydrodynamics model [3] can be used to estimate the initial energy density in such collisions. The Bjorken energy density ($\epsilon_{\rm Bj}$) with the assumption of boost invariance is given as [4–6],

$$\epsilon_{\rm Bj} \approx \frac{1}{\tau\pi R_0^2\left(\frac{N_{\rm part}}{2}\right)^{2/3}}\left[\frac{3}{2}\times\left(\langle m_{\rm T}\rangle\frac{dN}{dy}\right)_{\pi^\pm}+2\times\left(\langle m_{\rm T}\rangle\frac{dN}{dy}\right)_{K^\pm,p,\bar{p}}\right] \quad (1)$$

The multiplicative factors in each term account for corresponding neutral particles. The transverse mass and the integrated yield calculated for $\pi^\pm$, $K^\pm$ and $p+\bar{p}$ lie in the mid-rapidity region, *i.e.*, $|y| < 0.5$. The left and right plots of Fig. 1 depict the integrated yields and mean transverse momenta, respectively, for pions, kaons, and protons as a function of centrality classes for O+O collisions at $\sqrt{s_{\rm NN}}$ = 7 TeV. As expected, the integrated yield of pions is higher than that of kaons and protons, as pions are the most abundant of the identified particles. However, the mean transverse mass stays the same for both density profiles. With the input of integrated yields and mean transverse momenta, the Bjorken energy density is calculated using Eq. 1. The central collisions have a larger Bjorken energy density which linearly declines as one moves towards peripheral collisions as shown in the left side plot of Fig. 1. Bjorken energy density is highly dependent on integrated yield, as shown in Eq. 1. It reflects a similar trend as seen in integrated yields for various nuclear density profiles. The energy density of the oxygen nucleus with the HO is around 15% greater than that of the WS density profile. The α-C structure shows similar behavior to the HO density profile. However,

PoS(LHCP2022)305

the change is minimal for the peripheral collision system. It is to be noted that the initial energy density values for all collision centralities are larger than the predicted lattice QCD requirement of 1 GeV/fm^3 energy density for a deconfinement transition [7], which hints towards the possible QGP signals in O+O collisions at the LHC energy.

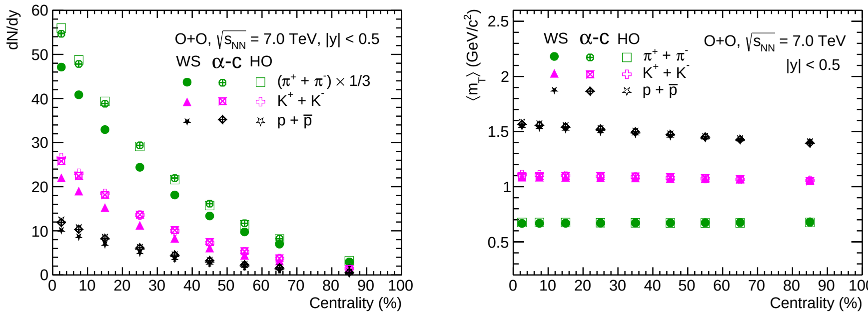

Figure 1: (Color online) Integrated yield (dN/dy) (left) and mean transverse mass ($\langle m_T \rangle$) (right) for pions, kaons, and protons in O+O collisions at $\sqrt{s_{\rm NN}}$ = 7 TeV as a function of centrality at mid-rapidity. The solid (open) markers represent the Woods-Saxon (harmonic oscillator) density profile, and markers with a cross represent α-clustered structure [8].

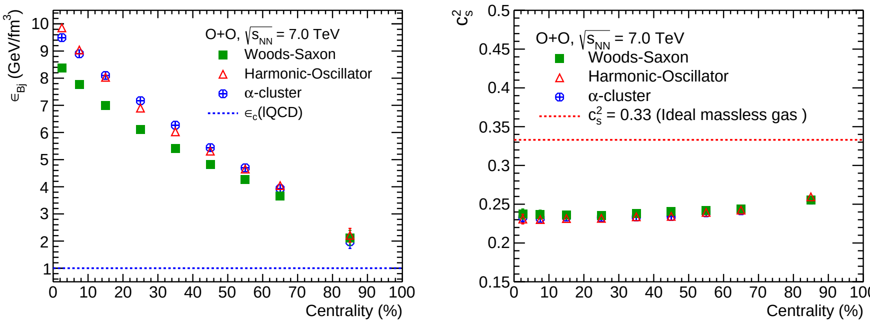

Figure 2: (Color online) Bjorken energy density (ϵ_{Bj}) (left) and squared speed of sound (c_s^2) (right) as a function centrality classes in O+O collisions at $\sqrt{s_{\rm NN}}$ = 7 TeV. The solid (open) markers represent the Woods-Saxon (harmonic oscillator) density profile, and markers with a cross represent α-clustered structure [8].

The squared speed of sound is related to the width of the pseudorapidity distribution, obtained by a double Gaussian fit, as shown in Eq. 2 [9–11].

$$\sigma_y^2 = \frac{8}{3}\frac{c_s^2}{1-c_s^2}\ln\left(\frac{\sqrt{s_{\rm NN}}}{2m_p}\right). \tag{2}$$

Where m_p is the proton's mass, and σ_y is the width of the pseudorapidity distribution. The right side plot of Fig. 2 shows the squared speed of sound as a function centrality in O+O collisions at $\sqrt{s_{\rm NN}}$ = 7 TeV for WS, HO and α-C structure of oxygen nucleus. Within the uncertainties, c_s^2 is found to be similar to a function of centrality. The red dashed line in the right plot of Fig. 2 represents the ideal gas limit, and the c_s^2 from O+O collisions is about 25% less than the ideal gas limit.

PoS(LHCP2022)305

Boltzmann-Gibbs blast-wave function (BGBW) [12] gives the estimation of kinetic freezeout temperature ($T_{\rm kin}$), and the mean transverse radial flow velocity ($\langle\beta_{\rm T}\rangle$) by a simultaneous fit to identified particles' transverse momentum spectra at the freezeout, defined as,

$$\left.\frac{d^2N}{dp_T dy}\right|_{y=0} = Cp_T m_T \int_0^{R_0} r\ dr\ K_1\Big(\frac{m_T\ \cosh\rho}{T_{\rm kin}}\Big) I_0\Big(\frac{p_T\ \sinh\rho}{T_{\rm kin}}\Big).$$

where, ρ is given by $\rho = \tanh^{-1}\beta_{\rm T}$ and $\beta_{\rm T}(=\beta_s\xi^n)$ [12–15] is the radial flow. Here, ξ is given as (r/R_0), β_s is the maximum surface velocity and r is the radial distance. Figure 3 shows the transverse radial flow versus kinetic freezeout temperature from a simultaneous fit of identified particles p_T-spectra with BGBW in O+O collisions at $\sqrt{s_{\rm NN}}$ = 7 TeV. $T_{\rm kin}$ is the lowest for the most central collisions (0-5%), and the transverse flow is the highest. Additionally, $\langle\beta_{\rm T}\rangle$ is the highest in the high multiplicity domain, *i.e.*, the most central collisions. At the LHC energy, Pb+Pb collisions exhibit a similar behaviour [16].

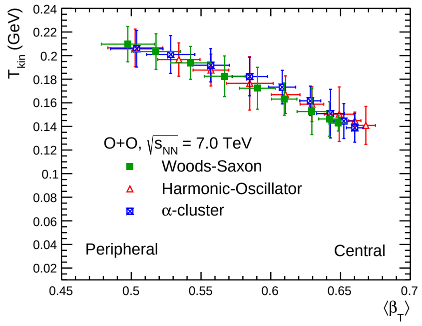

Figure 3: (Color online) Kinetic freezeout temperature versus transverse radial flow from simultaneous fit of identified particles' $p_{\rm T}$-spectra with Boltzmann-Gibbs blastwave distribution in O+O collisions at $\sqrt{s_{\rm NN}}$ = 7 TeV [8].

3. Summary

Here, we have predicted the global observables in O+O collisions at $\sqrt{s_{\rm NN}}$ = 7 TeV using the AMPT model. We report the charged-particle multiplicity at mid-rapidity, mean transverse mass, Bjorken energy density, squared speed of sound as a function of centrality, and the kinetic freezeout temperature dependency on mean transverse radial flow velocity. The initial energy density and charged-particle multiplicity for the α-C structure and HO density profile are found to be similar, whereas the squared speed of sound and the kinetic freezeout parameters are found to be independent of the type of the nuclear charged density profile.

Acknowledgements

D.B. acknowledges the financial support from CSIR, the Government of India. S.P. acknowledges the financial support from UGC, the Government of India. S.T. acknowledges the support under the INFN postdoctoral fellowship. Raghunath Sahoo acknowledges the financial support

PoS(LHCP2022)305

under the CERN Scientific Associateship, CERN, Geneva, Switzerland, and the financial grants under DAE-BRNS Project No. 58/14/29/2019-BRNS of the Government of India. A. N. M. thanks the Hungarian National Research, Development, and Innovation Office (NKFIH) under the contract numbers OTKA K135515, and NKFIH 2019-2.1.11-TET-2019-00078, 2019-2.1.11-TET-2019-00050 and the Wigner GPU Laboratory.

References

[1] J. Brewer, A. Mazeliauskas and W. van der Schee, arXiv:2103.01939 [hep-ph].

[2] Z. W. Lin, C. M. Ko, B. A. Li, B. Zhang and S. Pal, Phys. Rev. C **72**, 064901 (2005).

[3] J. D. Bjorken, Phys. Rev. D **27**, 140 (1983).

[4] R. Sahoo, A. N. Mishra, N. K. Behera and B. K. Nandi, Adv. High Energy Phys. **2015**, 612390 (2015) [erratum: Adv. High Energy Phys. **2017**, 4517153 (2017)].

[5] J. Adam *et al.* [ALICE Collaboration], Phys. Rev. C **94**, 034903 (2016).

[6] B. I. Abelev *et al.* [STAR Collaboration], Phys. Rev. C **79**, 034909 (2009).

[7] F. Karsch, Nucl. Phys. A **698** (2002), 199.

[8] D. Behera, N. Mallick, S. Tripathy, S. Prasad, A. N. Mishra and R. Sahoo, Eur. Phys. J. A **58**, 175 (2022).

[9] E. Abbas *et al.* [ALICE Collaboration], Phys. Lett. B **726**, 610 (2013).

[10] S. Prasad, N. Mallick, D. Behera, R. Sahoo and S. Tripathy, Sci. Rep. **12**, 3917 (2022).

[11] R. Sahoo, A. N. Mishra, N. K. Bahera and B. K. Nandi, Adv. High Energy Phys. **2015**, 612390 (2015).

[12] E. Schnedermann, J. Sollfrank and U. W. Heinz, Phys. Rev. C **48**, 2462 (1993).

[13] P. Huovinen, P. F. Kolb, U. W. Heinz, P. V. Ruuskanen and S. A. Voloshin, Phys. Lett. B **503**, 58 (2001).

[14] P. Braun-Munzinger, J. Stachel, J. P. Wessels and N. Xu, Phys. Lett. B **344**, 43 (1995).

[15] Z. Tang *et al.*, Chin. Phys. Lett. **30**, 031201 (2013).

[16] S. Acharya *et al.* [ALICE Collaboration], Phys. Rev. C **101**, 044907 (2020).

PoS(LHCP2022)305